High-temperature phase transition in a layered caesium-bismuth double molybdate: Raman study of lattice modes

1998 J. Phys.: Condens. Matter 10 8093

(http://iopscience.iop.org/0953-8984/10/36/017)

J. Phys.: Condens. Matter **10** (1998) 8093–8101. Printed in the UK PII: S0953-8984(98)94538-6

High-temperature phase transition in a layered caesium–bismuth double molybdate: Raman study of lattice modes

M Maczka†§, S Kojima† and J Hanuza‡

† Institute of Applied Physics, University of Tsukuba, Tsukuba, Ibaraki 305-8573, Japan
‡ Institute for Low Temperature and Structure Research, Polish Academy of Sciences, PO Box 937, 50-950 Wroclaw 2, Poland

Received 26 May 1998

Abstract. The Raman study of a single $CsBi(MoO_4)_2$ crystal has been performed in a 150–360 K temperature range. Three modes below 50 cm^{-1} at 150 K show remarkable softening as the temperature increases. The extrapolated values of these modes still exhibit finite frequency at the Curie point and they seem to be associated with the antiferro- to paraelectric phase transition.

1. Introduction

$CsBi(MoO_4)_2$ is a member of the family of layered double tungstates and molybdates. Among this family, with the general formula $M^I M^{III}(M^{VI}O_4)_2$, ferroelastic phase transitions have been found for trigonal compounds where M^I = Na, K, Rb, Cs; M^{III} = Al, In, Sc and M^{VI} = Mo, W [1]. $CsBi(MoO_4)_2$ belongs to the second group of orthorhombic crystals with M^I = K, Cs; M^{III} = Dy, Bi, Pr, Er and M^{VI} = Mo, W. In this group caesium–dysprosium double molybdate has been the most extensively studied and a second-order phase transition was discovered at 50 K followed by a first-order cooperative Jahn–Teller phase transition at 42 K [2]. Two phase transitions have been found also in $CsBi(MoO_4)_2$: a second-order one at 325–330 K and a first-order ferroelastic transition at around 145 K [3–6]. According to the results of Brilingas *et al* the second-order phase transition occurs between para- and antiferroelectric phases and above the Curie point T_C the ε_{33} component of the dielectric permittivity follows the Curie–Weiss law with the Curie constant 0.3×10^5 K [4]. The crystal structure of the paraelectric phase is the same as that of $CsPr(MoO_4)_2$ and $CsDy(MoO_4)_2$ i.e. $D_{2h}^3 = Pccn$ with two molecules in the unit cell [7]. The crystal structure below T_C has been not yet determined and it is still not clear whether the transformation is associated with a multiplication of the unit cell. In this paper, the temperature dependence of the lattice modes studied by the Raman technique is presented for the first time. We discuss the polarization dependence of lattice modes and we propose the assignment of the observed modes to the respective motions of ions in the unit cell. Finally, we discuss the possible structural changes occurring in the crystal at the 325 K phase transition.

§ On leave from: Institute for Low Temperature and Structure Research, Poland.

0953-8984/98/368093+09$19.50

2. Experiment

Single crystals were grown by the thermal method developed by Klevtsov *et al* [8] with the cooling rate 2 K per hour. Back-scattering Raman spectra were obtained with a triple-grating spectrometer of additive dispersion (Jobin Yvon, T64000) with a spectral resolution of 2 cm^{-1}. The output signal from the spectrometer was detected by the photon counting technique. The excitation source was the 514.5 nm line of an Ar-ion laser.

3. Selection rules for the paraelectric D_{2h}^3 structure

Before we discuss the changes observed in the lattice mode region induced by the 325 K phase transition, it is very important at first to established the number of lattice modes for the paraelectric phase. The knowledge of their polarization dependence should help us to assign the observed bands to the respective translational and librational motions of ions in the unit cell. If then we were able to attribute the observed changes in the spectra, induced by the phase transition, to specific motions of some ions in the unit cell, it would give us an insight into the transition mechanism.

The D_{2h}^3 structure is built up of layers formed of MoO_4^{2-} tetrahedra, situated on a mirror plane, connected to Bi^{3+} ions located at sites of D_2 symmetry. These layers are weakly bonded to caesium ions located at sites of D_2 symmetry. A total of 36 ($\boldsymbol{k} = 0$) lattice unit cell modes are distributed among $B_{1u} + B_{2u} + B_{3u}$ acoustic modes, $A_g + B_{1g} + 2B_{2g} + 2B_{3g} + 2A_u + 2B_{1u} + B_{2u} + B_{3u}$ librational modes and $2A_g + 4B_{1g} + 3B_{2g} + 3B_{3g} + A_u + 2B_{1u} + 3B_{2u} + 3B_{3u}$ translational modes. The translational Raman active modes may be further subdivided into translational movements of molybdate tetrahedra ($2A_g + 2B_{1g} + B_{2g} + B_{3g}$), translations of caesium ions ($B_{1g} + B_{2g} + B_{3g}$) and translations of bismuth ions ($B_{1g} + B_{2g} + B_{3g}$). In the present study Raman spectra have been recorded for the $x(yy)\bar{x}$ and $x(zz)\bar{x}$ polarization configurations, in which only A_g modes should be observed, and for $x(yz)\bar{x}$ polarization to record the B_{3g} modes. Note that translational modes of both Bi^{3+} and Cs^+ ions are inactive for A_g configuration, therefore only three A_g modes are expected to be observed in the lattice mode region.

4. Results and discussion

4.1. Assignment of lattice modes above T_C

The recorded spectra at 360 K are presented in figure 1. At this temperature the vibrational bands are very broad, possibly due to some disorder or defects. Four modes are observed for the A_g polarization configuration instead of only three. Such behaviour may be explained as a result of distortion from the D_{2h}^3 structure which is most likely caused by symmetry-breaking defects produced in the crystal at higher temperature. It was observed earlier that heating of $CsBi(MoO_4)_2$ crystal leads to creation of defects with very long relaxation time [6]. These defects are probably due to oxygen vacancies. However, although the spectra are not fully polarized, the two bands at 220 and 151 cm^{-1} may be unambiguously assigned to the translational movements of molybdate ions and that at 80 cm^{-1} to the librational motions. For the $x(yz)\bar{x}$ polarization five bands are observed at 242, 180, 151, 68 and 54 cm^{-1}. The 151 cm^{-1} band has been already assigned as A_g mode, therefore only four B_{3g} modes are observed out of five predicted. The missing mode may be probably located at 107 cm^{-1} since this mode at 294 K temperature shows most of its intensity in the $x(yz)\bar{x}$ configuration. Unlike the A_g symmetry modes, which originate in pure motions of MoO_4^{2-} tetrahedra, for

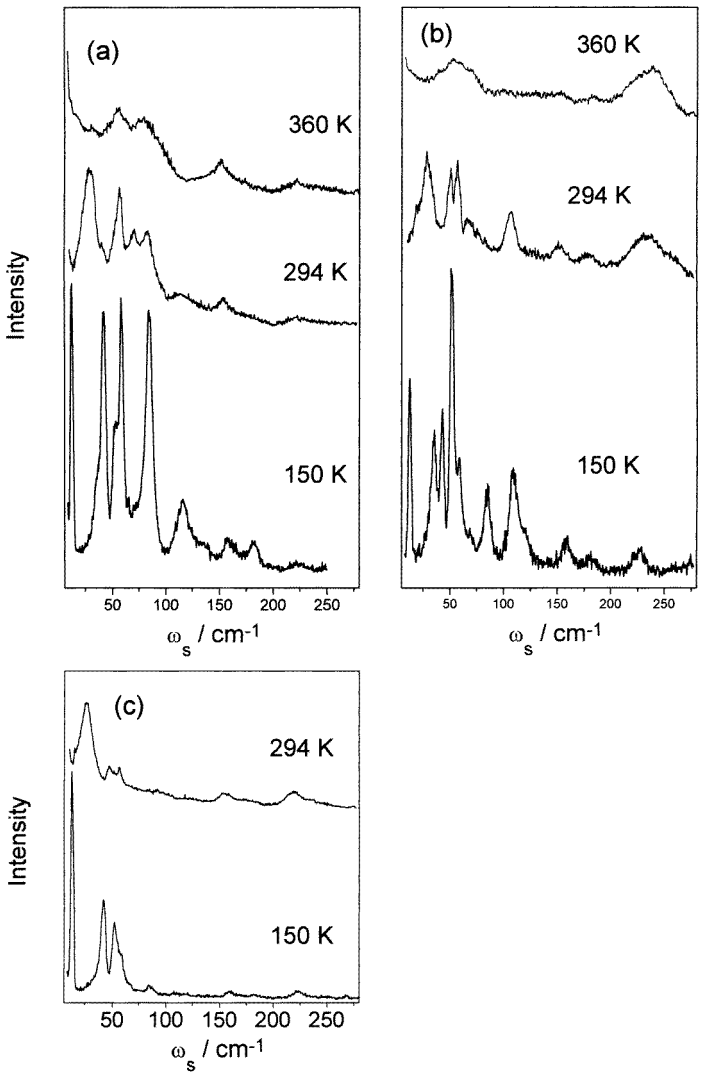

Figure 1. The Raman spectra of $CsBi(MoO_4)_2$ at 360, 294 and 150 K temperature: (a) $x(zz)\bar{x}$ polarization, (b) $x(yz)\bar{x}$ polarization and (c) $x(yy)\bar{x}$ polarization.

the $x(yz)\bar{x}$ configuration both librations and translations of all ions are allowed by symmetry and therefore coupling between the same symmetry modes may occur. This coupling is probably very weak in the case of weakly bonded Cs^+ ions but may be significant for the strongly bonded MoO_4^{2-} and Bi^{3+} ions. Our earlier study of trigonal layered crystals has shown that translational modes of heavy Cs^+ ions should be observed below 100 cm^{-1} [9]. We have also shown that for layered compounds the coupled intralayer modes, i.e. $T'(M^{3+})*T'(MoO_4^{2-})$, have been observed at about 200 cm^{-1} for indium compounds [9]. Since the frequency of a translational vibration is approximately proportional to the square root of the appropriate reciprocal reduced mass [10], replacing In^{3+} ions (atomic mass 115) by heavier Bi^{3+} ions (atomic mass 209) should cause a frequency decrease. Such a comparison between two crystals belonging to different groups is justified because the

intralayered force constants in both cases are similar as has been shown by normal coordinate analysis of a few trigonal and orthorhombic crystals [11]. The above considerations allow us to conclude that the bands at 242 and 180 cm^{-1} are due to the coupled translational motions of bismuth and molybdate ions, the first one involving mainly molybdate and the second mainly bismuth ion motions. The two bands at 107 and 54 cm^{-1} may be assigned to the librational movements and the weak band at 66 cm^{-1} to the $T'(Cs^{+})$.

The recorded spectra at 294 and 150 K temperatures are presented together with those measured at 360 K in figure 1 and the observed wavenumbers are summarized in table 1. In the region 55–280 cm^{-1} no additional band appears at 150 K as compared with 360 K. The measured bands show only minor frequency changes but some of them show significant intensity changes. For example, the 181 and 107 cm^{-1} modes, observed mainly for the $x(yz)\bar{x}$ polarization at ambient temperature, become stronger for the $x(zz)\bar{x}$ polarization at 150 K. Similarly, the 80 cm^{-1} mode observed for the $x(zz)\bar{x}$ polarization becomes visible also for the $x(yz)\bar{x}$ polarization at low temperature. Since those modes involve the motions of molybdate ions such behaviour clearly indicates that the crystal distortion due to the phase transition leads to the lowering of the point group symmetry of MoO_4^{2-} tetrahedra from C_s to C_1 and therefore allows the modes, which were originally only A_g or B_{3g} active, be observed for both polarizations.

Table 1. Vibrational lattice modes of $CsBi(MoO_4)_2$ crystal at different temperatures and polarizations.

360 K		294 K			150 K			
$x(zz)\bar{x}$	$x(yz)\bar{x}$	$x(yy)\bar{x}$	$x(zz)\bar{x}$	$x(yz)\bar{x}$	$x(yy)\bar{x}$	$x(zz)\bar{x}$	$x(yz)\bar{x}$	Assignment
237vw	242w	236vw		234w			226vw	$T'(MoO_4)$*$T'(Bi^{3+})$
220w		219m	222w		223vw	223vw		$T'(MoO_4)$
	180vw	176vw		180vw	182vw	182w	181vw	$T'(MoO_4)$*$T'(Bi^{3+})$
151w	151vw	155m	154w	153vw	159vw	159vw	158vw	$T'(MoO_4)$
			110w	107w	107vw	115m	108w	$L(MoO_4)$
80m			82m		85m	84s	85w	$L(MoO_4)$
	68sh		67vw	66vw	69vw			$T'(Cs^{+})$
54w	54w	56m	57m	57w	58sh	58s	59vw	$L(MoO_4)$
		48m		50w	52s	52sh	52m	?
		27vs	27m	27w	42s	42s	43m	soft mode
						35sh	35m	soft mode
					13vs	12s	13m	soft mode

vw—very weak; w—weak; m—medium; s—strong; vs—very strong; sh—shoulder.

4.2. Low-frequency modes below 55 cm^{-1}

The phase transition leads to the appearance of four new modes in the wavenumber region below 55 cm^{-1}. The mode at about 50 cm^{-1}, showing most of its intensity in the $x(yy)\bar{x}$ polarization, shows very slight frequency increase with decreasing temperature (2 cm^{-1} between 294 and 150 K). The remaining modes, two very strong of A_g symmetry observed at 43 and 13 cm^{-1} at 150 K, and one weak of B_{3g} symmetry at 35 cm^{-1}, show remarkable softening with increasing temperature. Since the weak 35 cm^{-1} band at higher temperature becomes completely obscured by the much stronger 43 cm^{-1} band, we have extracted the temperature dependence of the mode frequency and line-width only for the two modes at 43 and 13 cm^{-1}, recorded for the $x(yy)\bar{x}$ polarization (figure 2). For this configuration the

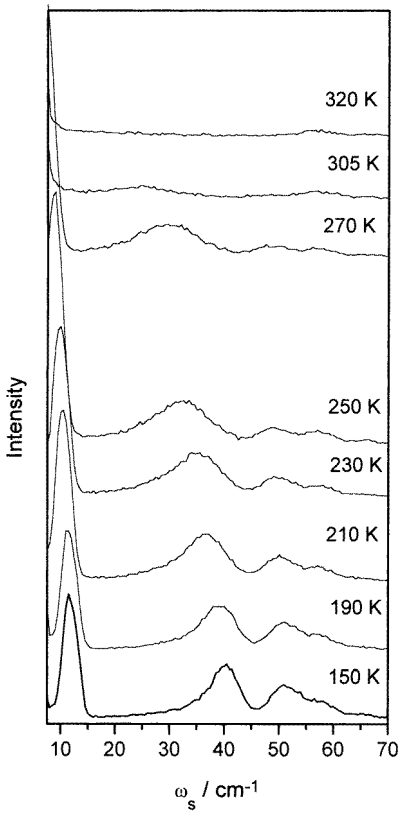

Figure 2. The Raman spectra of $CsBi(MoO_4)_2$ at different temperatures measured for the $x(yy)\bar{x}$ polarization configuration.

B_{3g} mode is almost inactive and the two other modes are very strong. In the case of the 13 cm^{-1} line the results are presented only up to 270 K. Above this temperature the line cannot be observed since it is hidden in increasing Rayleigh wing. The appearance of the Rayleigh wing is another proof of the increasing number of defects at elevated temperatures. In the temperature range studied this mode is underdamped and therefore its frequency, linewidth and integrated intensity were extracted from fitting to the Lorentzian band shape. The 43 cm^{-1} soft mode becomes overdamped near the Curie point and therefore the line shape was fitted to a damped oscillator model given by:

$$I(\omega) = [n(\omega) + 1]S\omega\Gamma\omega_s^2/[(\omega_s^2 - \omega^2) + \omega^2\Gamma^2] \tag{1}$$

where $I(\omega)$ is the intensity of the spectrum, $n(\omega) = 1/[\exp(h\omega/k_BT) - 1]$ is the Bose–Einstein factor, S, ω_s and Γ are the oscillator strength, frequency and half-width of the soft mode, respectively. The obtained values of $\omega_s, \omega_s^2, \Gamma$ and integrated intensity (or oscillator strength) are plotted as a function of temperature in figures 3–6. At $T < T_C$ the temperature dependence of the squared frequency of the modes is obtained by a least squares fitting, which is described by $\omega_s^2 = 0.96(T_C - T)^{0.97} + 16.2$ for the 13 cm^{-1} and by $\omega_s^2 = 7.48(T_C - T)^{0.98} + 558$ for the 43 cm^{-1} soft mode, showing that ω_s^2 decreases linearly with increasing temperature in both cases and that both modes have a finite frequency at T_C. The finiteness of ω_s at T_C seems to be a characteristic feature of many bismuth

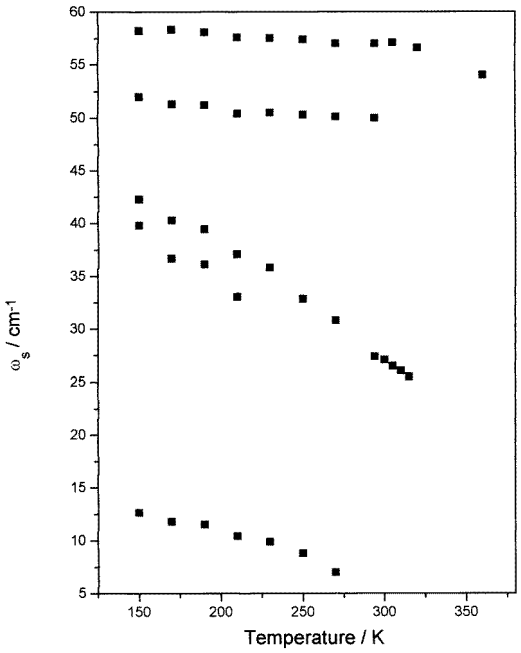

Figure 3. The temperature dependence of the frequency of the lattice modes below 60 cm^{-1}.

layered compounds. For example, finite frequencies have been found for $Bi_4Ti_3O_{13}$ [12] and $Bi_2Ti_4O_{11}$ [13] compounds. In the latter publication the authors could show that the finiteness of ω_s at T_C originated from a coupling of the soft optical mode to an additional mode which might be a zone boundary mode.

The temperature dependence of the 13 cm^{-1} phonon damping (Γ) could not be established since the observed changes were very small. At 150 K the half-width was only 2.69 and at 250 K 2.85 cm^{-1}. The temperature dependence of the 43 cm^{-1} soft mode damping is anomalous (see figure 5). The plot of damping as a function of temperature shows that it can be divided into two regions. In the 150–250 K temperature region the temperature dependence of the phonon damping can be fitted with the formula [14]:

$$\Gamma = A + BT + CT^2 \tag{2}$$

where T is temperature, and A, B, C are constants. The first term denotes damping due to scattering at defects. The second and third terms represent damping caused by scattering due to third- and fourth-order anharmonicity, respectively. The obtained values of A, B and C are: 3.65, -0.022 and 2.24, respectively. Above 290 K this mode becomes overdamped and the line-width increases quickly with the increasing temperature.

The calculated oscillator strength of the 43 cm^{-1} soft mode also shows an anomaly. It increases with the increasing temperature up to 230 K and decreases linearly in the region 230–320 K. A least squares fitting to the data above 230 K gives the transition temperature of 322 K, in good agreement with the heat capacity study, where this temperature was estimated at 325 K [6]. The plot of the integrated intensity (divided by $n(\omega) + 1$, where $n(\omega)$ is the Bose–Einstein factor) of the 13 cm^{-1} line as a function of temperature shows, surprisingly, that although this mode softens its intensity begins to decrease probably close to the phase transition temperature. This mode together with the A_g mode at 43 and the

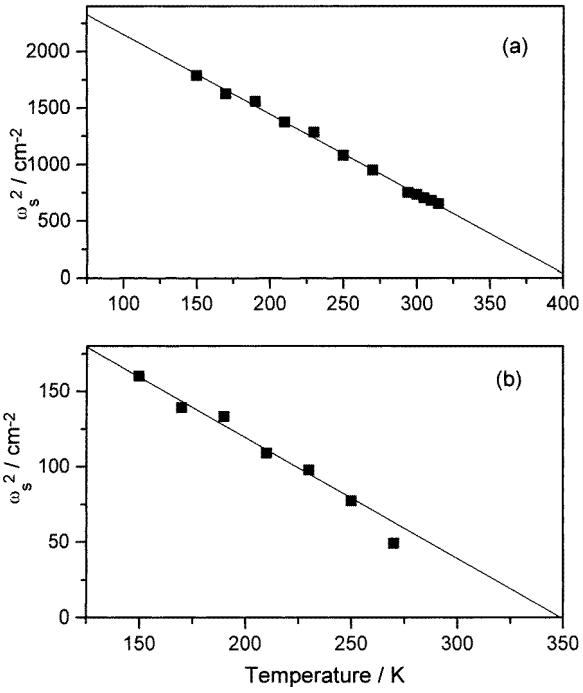

Figure 4. The squared frequency of the 43 cm^{-1} mode (a) and the 13 cm^{-1} mode (b).

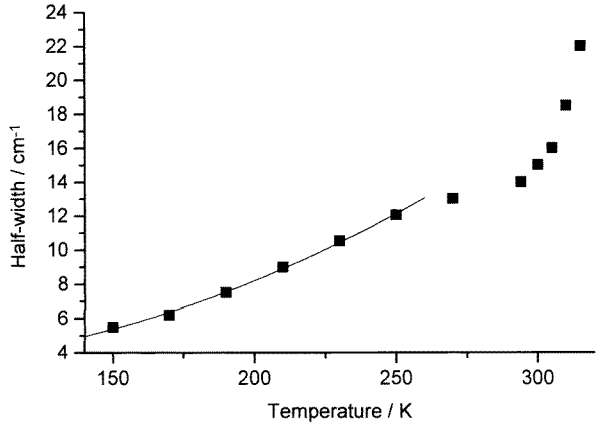

Figure 5. The temperature dependence of the half-width of the 43 cm^{-1} mode. The solid line is a curve fitted by equation (2) to the data in the 150–230 K temperature range.

B_{3g} mode at 35 cm^{-1} may be most probably assigned to the Brillouin zone boundary soft mode of the antiferroelectric transition from the paraelectric phase. Its origin is most likely the same as the 8.2 cm^{-1} line found below 50 K in the $CsDy(MoO_4)_2$ crystal [2]. For the dysprosium crystal the intense line flared up at the second-order phase transition (50 K) and then showed slow intensity decrease with decreasing temperature. The similarity of Raman spectra below the phase transition temperature recorded for $CsBi(MoO_4)_2$ and

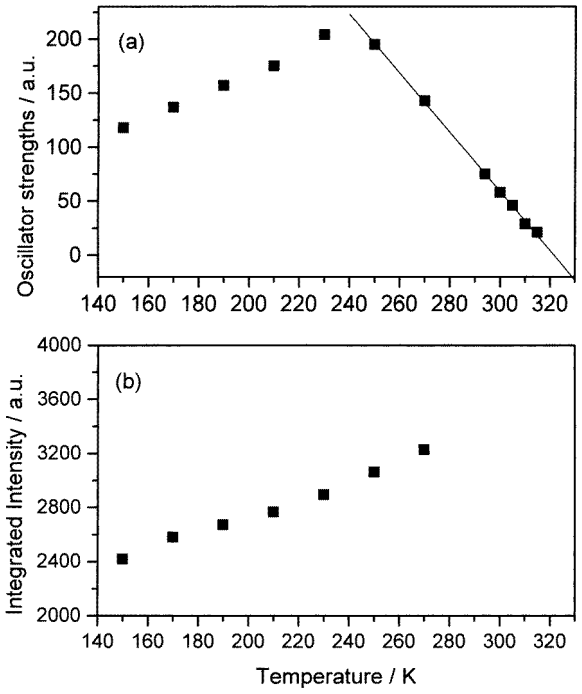

Figure 6. (a) The oscillator strength of the 43 cm^{-1} mode as a function of temperature. The solid line is a curve fitted with the formula $S = A + BT$, where S denotes oscillator strength and T is temperature. (b) Integrated intensity of the 13 cm^{-1} mode as a function of temperature.

$CsDy(MoO_4)_2$ permits the assumption that the mechanism of these transitions is similar for both double molybdates. However, in the case of the dysprosium crystal no observation of soft modes has been reported, probably because of a very narrow temperature range in which the discussed phase exists (only 8 K for $CsDy(MoO_4)_2$ and 24 K for $CsDy_{0.93}Gd_{0.07}(MoO_4)_2$ crystal [2]).

5. Conclusion

The results of the present investigation combined with the results obtained for $CsDy(MoO_4)_2$ and $CsDy_{0.93}Gd_{0.07}(MoO_4)_2$ crystals permit us to draw the following conclusions:

- The phase transition at 325 K seems to be displacive and of second order with the exponent $\beta = 0.5$.
- This transition is driven by three zone boundary soft modes, observed at 43, 35 and 13 cm^{-1} at 150 K, and the low-temperature unit cell doubles along the $\boldsymbol{a}$ axis i.e. contains two layers (four formula units). The point symmetry of MoO_4^{2-} tetrahedra lowers from C_s to C_1.
- If we assume that the phase transition mechanism is similar to that of the isostructural dysprosium compound, this transition is not driven by the displacements of the bismuth sublattice, since the Raman investigation of caesium–dysprosium double molybdate doped with gadolinium ions showed that the transition was not affected by the gadolinium impurity.

Finally, we may conclude that the discussed transformation seems to be associated

with the antiferro-distortive motions of molybdate ions and probably also with translational motions of caesium ions. However, the results of the Raman study do not permit us to describe the symmetry of the low temperature structure. We may only conclude that the possible structure might be also orthorhombic since in the case of monoclinic distortion the eight molybdate ions in the unit cell would have to occupy two crystallographically non-equivalent sets and therefore more lines should be observed than we were able to measure in the present study.

Acknowledgments

This work was partially supported by the Foundation for Advancement of International Science and the Polish State Committee for Scientific Research, grant No PB 755/TO9/97/13. One of the authors (Miroslaw Maczka) acknowledges the Japanese Society for the Promotion of Science for the financial support of his stay at University of Tsukuba.

References

[1] Otko A I, Pelich L N, Povstyanyi L V, Nesterenko N M, Kalinin P S and Zvyagin A I 1975 *Izv. Akad. Nauk SSSR, Ser. Fiz.* **39** 697
[2] Fomin V I, Gnezdilov V P, Eremenko V V and Nesterenko N M 1989 *Sov. Phys.–Solid State* **31** 871 and references therein
[3] Pelich L N and Zvyagin A I 1978 *Sov. Phys.–Solid State* **20** 1106
[4] Brilingas A, Grigas I, Gurskas A, Zvyagin A I, Kalesinskas V and Pelich L N 1980 *Sov. Phys.–Solid State* **22** 2039
[5] Zvyagin A I and Kutko V I 1987 *Fiz. Nizkih. Temp.* **13** 537
[6] Stokka S and Samulionis V 1981 *Phys. Status Solidi* a **67** K89
[7] Klevtsov P V, Vinokurov V A and Klevtsova R F 1973 *Kristallografiya* **18** 1192
[8] Klevtsov P V, Kozeeva L P and Khartzenko L Yu 1975 *Kristallografiya* **20** 1210
[9] Maczka M 1996 *Eur. J. Solid State Inorg. Chem.* **33** 783
[10] Nicol M and Durana J F 1971 *J. Chem. Phys.* **54** 1436
[11] Fomichev V V and Kondratov O I 1992 *Zh. Neorg. Khim.* **37** 1165
[12] Kojima S and Shimada S 1996 *Physica* B **219/220** 617
[13] Meng J, Zou G, Cui Q and Ma Y 1994 *Phys. Status Solidi* a **144** 353
[14] Silverman B D 1962 *Phys. Rev.* **125** 1921